Studies on γ-Fe_2O_3–High-Density Polyethylene Composites and Their Additives

B. Govindaraj,[1] N. V. Sastry,[2] A. Venkataraman[3]

[1]*Department of Chemistry, Vijayanagar College, Hospet-583 201, India*
[2]*Department of Chemistry, Sardar Patel University, Vallabh Vidyanagar, Gujarat, India*
[3]*Department of Chemistry, Gulbarga University, Gulbarga 585 106, India*

Received 11 June 2003; accepted 25 September 2003

ABSTRACT: γ-Fe_2O_3–high-density polyethylene (HDPE) composite films are prepared by a gel-casting technique. To understand the effect of additives, rice husk ash and thiourea are made to disperse in the HDPE matrix to obtain the composite films with additives. The as-prepared γ-Fe_2O_3–HDPE composite films with their additives are subjected to characterization and study through X-ray diffraction, thermal, scanning electron microscopy, and dielectric measurements. The results are qualitatively treated. © 2004 Wiley Periodicals, Inc. J Appl Polym Sci 92: 1527–1533, 2004

Key words: magnetic polymers; composites; additives; morphology; structure; thermal behavior

INTRODUCTION

Nanomaterials consist of particles with a diameter less than 100 nm and they exhibit special physical, thermal, magnetic, or mechanical properties related to this small dimension. A nanocomposition is a material composed of two or more phases, one of which has a grain size of less than 100 nm. Here the combination of different physical or chemical properties may lead to completely novel materials. The grain size limit of 100 nm is general, but most phenomena related to grain size are restricted to particles with sizes below 10 nm. Since the pioneering work of Gleiter,[1–3] many research groups have contributed to the synthesis[4–9] and property evaluation[10–16] of nanomaterials and nanocomposites. Several methods of synthesis, such as inert gas condensation,[4,5] the sol-gel process of microwave plasma processing,[6–9] were developed to produce nanomaterials.

Except for properties related to grain boundaries,[10,11] most of the physical properties of interest are those of noninteracting isolated particles.[12–16] Such properties can be measured in extremely dilute suspensions. For technical applications, one needs a dense body composed of nanoparticles that can be handled while still exhibiting the special "nano" properties. Even when the sintering activity of compacted nanoparticles is high, standard procedures of powder metallurgy, such as pressing and sintering, are almost impossible to perform if the material is to retain its nano properties. The main reason for this is that the grain growth occurs during sintering or heat treatment, increasing the particle size (up to a few hundred nanometers). Thus, the properties related to the small grain size are lost. Moreover, many of these special properties stem from isolated particles. In a sintered body, even at the right grain size, the particles interact. In many cases this destroys the intended special properties.

Nanocomposites can solve these problems. In an ideal nanocomposite, which is similar to a suspension, the active nanoparticles (i.e., the carriers of the desired property) are well separated. Theoretically, the mechanical blending of two or more powders could produce such composites. However, due to the aggregation of nanoparticles by van der Waals forces, such processes never lead to isolated particles. The application of wet chemical methods is better, but not always successful. The best way to solve the problem is to coat the nanoparticles. The coating must be applied before the particles get a chance to agglomerate by van der Waals forces.

Polymer nanocomposites are materials in which nanoscopic inorganic particles, typically 10–100 nm in at least one dimension, are dispersed in an organic polymer matrix to dramatically improve the performance properties of the polymer. Systems in which the inorganic particles are the individual layers of a lamellar compound, most typically a smectite clay or nanocomposites of a polymer (such as nylon) embedded among layers of silicates when produced exhibit dramatically altered physical properties relative to the pristine polymer. For instance, the layer orientation,

Correspondence to: A. Venkataraman (venkat95@sancharnet.in).

Journal of Applied Polymer Science, Vol. 92, 1527–1533 (2004)

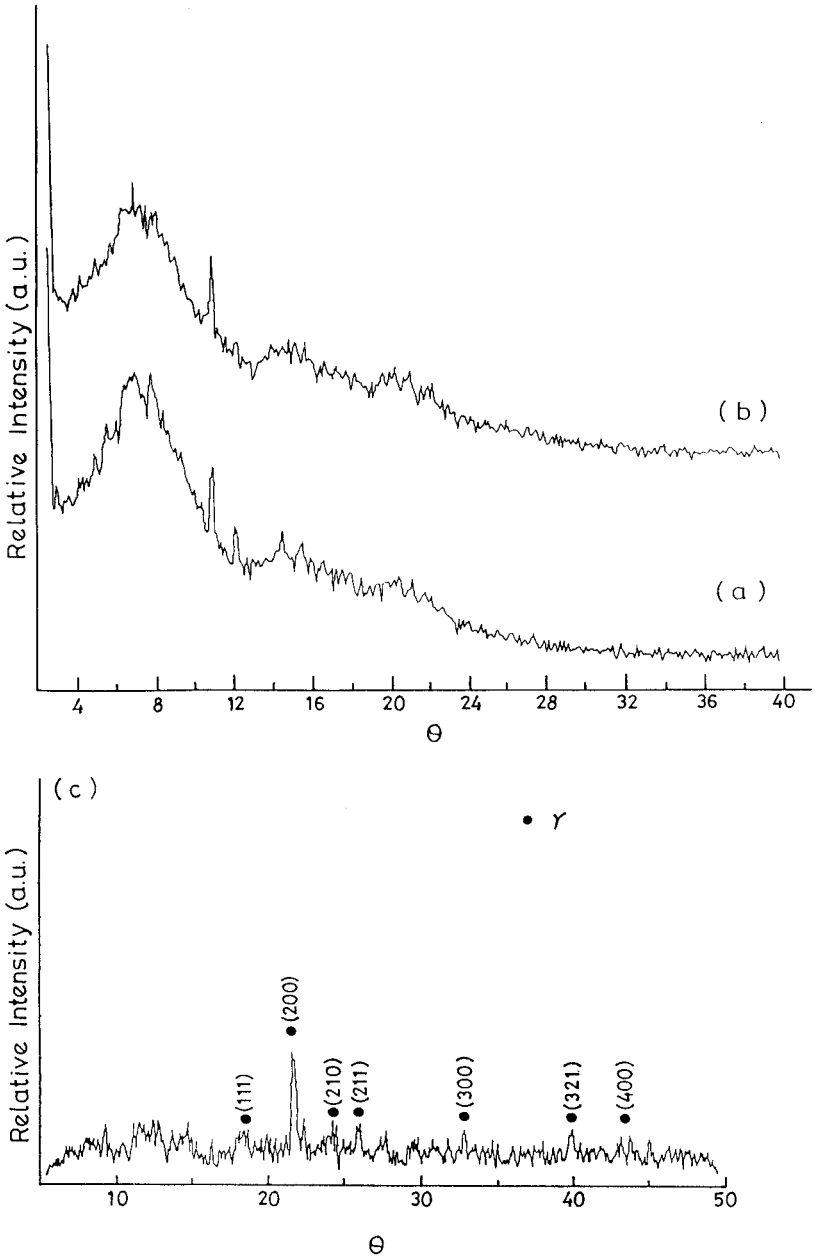

Figure 1 XRD patterns of (a) HDPE (PE) film, (b) PEA composite film, (c) PEG composite film, (d) PEGA composite film, (e) PETUG composite film, and (f) PETUGA composite film.

stiffness, strength, and dimensional stability in two dimensions (rather than one) are the specific features of polymer–silicate nanocomposites. In addition, because the length scale involved is the one which minimizes the scattering, nanocomposites are usually transparent. Furthermore, the nanocomposites of polymer-layered silicate (PLS) exhibit a significant increase in thermal stability as well as self-extinguishing characteristics. Polyolefin nanocomposites have been successfully made by compounding, resulting in well-exfoliated and dispersed nanofillers in the polyolefin matrix.[17] Nylon nanocomposites and their significance have also been reported.[18–20] The effect of adding fillers and additives was studied to some extent on polyethylene.[21,22] There was a good deal of interest in the study of polyethylene in the 1960s through the 1970s.[21–25] These additives help to increase the mechanical strength, thermal stability, etc., of the polymer matrix. The effects of nonmagnetic additives on polyethylene matrix are reported in literature to some extent.[26]

Continuing our investigations studying ferrite composites with conducting and nonconducting polymers, in the present study a commercially available high-density polyethylene was used to prepare the high-density polyethylene (HDPE)–γ-Fe_2O_3 compos-

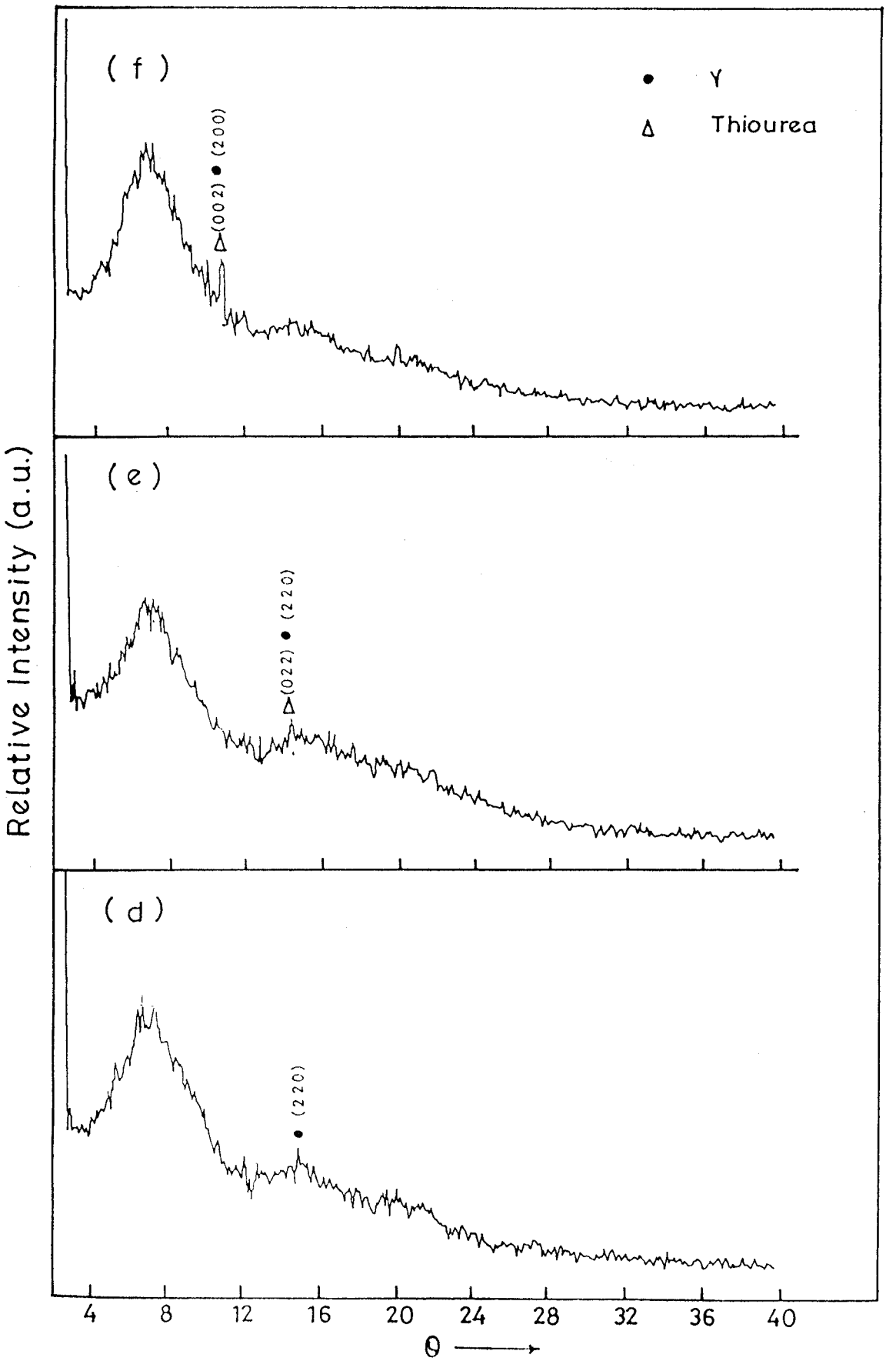

Figure 1 (*Continued from the previous page*)

ite films. The prepared films are characterized. We also aim at understanding the effects on the crystallinity, thermal, and structural features of HDPE–ferrite composites. The effect of nonmagnetic additives such as rice husk ash and thiourea was also monitored.

EXPERIMENTAL

The HDPE is of commercial origin and was obtained as gift sample from Nocil (Mumbai, India). The γ-Fe_2O_3 was prepared by employing ferrous succinate tetrahydrate precursor through a self-propagated combustion reaction similar to that reported elsewhere.[27,28] The complex composite thiourea–γ-Fe_2O_3 (TUG) was also prepared as reported earlier.[29,30]

Preparation of γ-Fe_2O_3–HDPE composite film

The polymer composite films were thus prepared by a gel-casting technique. One gram of high-density polyethylene was dissolved in 50 mL of xylene to make it a gel. To this gel 0.1 g (10% by weight) of pure γ-Fe_2O_3 was added and the suspension was stirred continuously over a temperature range 60–80°C. The gel then was immediately transferred into a petri dish and the solvent was allowed to evaporate over a period of 24 h. After all the solvent was evaporated, a thin film of γ-Fe_2O_3–HDPE was peeled off by gently spraying distilled water into the petri dish.

Preparation of processed rice husk ash (A)

Rice husk from the local rice mill was treated with nitric acid under constant stirring. The mixture was kept for 24 h to remove excess oxides and impurities from the husk. Then the mixture was filtered, washed with deionized water, and dried. This treated husk was finely ground and ignited in a silica crucible kept in an electric oven. A colorless and weightless powder was finally obtained. Heating and weighing were repeated to a constant weight. This powdered rice husk ash (A) was used as one of the nonmagnetic additives in HDPE–ferrite nanocomposites.

Preparation of γ-Fe_2O_3–polymer composite films with additives

The polymer composite films had been prepared with HDPE along with rice husk ash (A) and the TUG complex separately. The composite films were also prepared by employing the same gel casting technique as employed to prepare HDPE films. Here a known weight of the polymer (HDPE) was made into gel by dissolving in solvent xylene. To this gel a known weight (10% by weight) of the additives (rice husk ash/thiourea) was added, and the mixture was sonicated for 2 h and then subjected to solvent evaporation. Fine transparent films were obtained. Even though all the composite films of HDPE with varying compositions of the additives (2, 5, and 10% by weight) were prepared, only those composite films with HDPE and 10% by weight of the additives are reported here because they showed uniform dispersion of the additives in the HDPE matrix.

The film samples were abbreviated as follows: the dispersed γ-Fe_2O_3 sample in the HDPE matrix was taken out as thin films (PEG) through a gel casting technique. Similarly, a chemically treated rice husk ash (A) was also dispersed in the HDPE matrix and obtained as films (PEA). A mixture of (A) and (γ-Fe_2O_3) in the ratio 1:1 by weight was also dispersed in the HDPE matrix to get thin films (PEGA). By following the same procedure HDPE composite films like PETUG (by dispersing TUG in HDPE matrix) and PETUGA (by dispersing the mixture of TUG and Ash(A) in the weight ratio of 1:1 into the polymer matrix HDPE) were prepared. The as-prepared HDPE composite films were subjected to characterization and studies, wherein the similarities were observed. Only the representative figures and data are presented in this paper.

RESULTS AND DISCUSSIONS

X-ray diffraction study

X-ray diffraction patterns (XRD) of pure HDPE (PE), PEA, PEG, PEGA, PETUG, and PETUGA are shown in Figure 1a–f, respectively. Figure 1a represents the XRD pattern of pure HDPE (PE) film. It shows some crystallinity in its nature along with a broad region due to polymeric amorphosity. Figure 1b represents the XRD pattern of processed rice husk ash (A) dispersed in the HDPE matrix (PEA). This pattern resembles that of pure HDPE with a slight increase in its amorphosity, possibly due to the presence of ash, which is amorphous in nature. The peak at *d* value of 3.7049 Å has been slightly shifted, indicating the interaction of ash particles with the polyethylene matrix. Figure 1c represents the XRD pattern of γ-Fe_2O_3 dispersed in HDPE (PEG). Upon comparison with the XRD of pure HDPE, an increase in crystallinity was observed, with the peaks at *d* values of 4.814, 4.099, 3.693, 3.444, 2.730, 2.249, and 2.087 Å with Miller indices (111), (200), (210), (211), (300), (321), and (400) confirming the presence of γ-Fe_2O_3 (ASTM File No. 04–755) dispersed in the PE matrix.

Figure 1d represents the XRD pattern of PEGA. Here there is a clearly observed γ-Fe_2O_3 peak at *d* value 3.0013 Å with Miller index (200), which matches with ASTM File No. 04–755. Iit is also observed that a broad curve in PEA due to the presence of ash is now slightly sharpened in PEGA because of an increase in

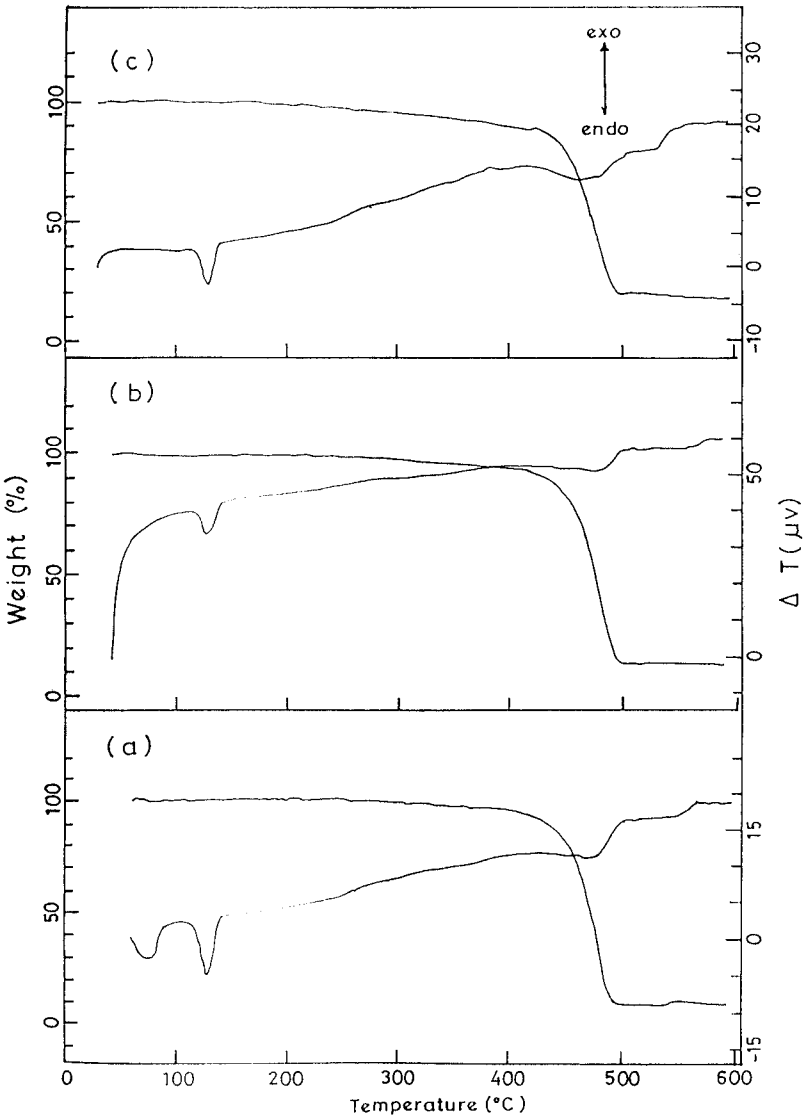

Figure 2 TGA/DTA traces of (a) PEG composite film, (b) PEGA composite film, and (c) PETUGA composite film

its crystalline nature. This is possibly due to the presence of γ-Fe_2O_3 particles uniformly dispersed throughout the HDPE matrix.

Figure 1e represents the XRD pattern of PETUG. This figure shows the peak at *d* value 3.0990 Å, which confirms the presence of both γ-Fe_2O_3 with Miller index (220) and thiourea with Miller index (022). These match with ASTM File No. 04–755 and JCPDS File No. 03–0235, respectively. Upon comparison with the XRD pattern of pure HDPE, it is observed that the decrease in amorphosity of polymer is noted by the sharpening of the diffraction pattern in the region.

Figure 1f represents the XRD pattern of PETUGA. This figure shows the presence of both γ-Fe_2O_3 and thiourea at the *d* value 4.1019 Å with Miller indices (200) and (002), respectively. This is in accordance with ASTM File No. 04–755 (for γ-Fe_2O_3) and JCPDS File No. 03–235 (for thiourea), respectively. In this figure we again observe the broadening of the polymer region because of the presence of amorphous ash dispersed in the HDPE matrix. The above results confirm that, due to the presence of γ-Fe_2O_3 and thiourea, the crystallinity increases and due to the presence of ash crystallinity decreases for the HDPE matrix.

Thermal study

Figure 2a–c shows the thermal behavior of HDPE composite films. Figure 2a represents the TGA/DTA trace of PEG. This trace shows a weight loss of 9% in the region of 74–430°C(I step of weight loss). This weight loss is quite slow. Later continuous weight loss is observed in the temperature region of 430–589°C, showing a maximum of 82%. At 589°C a residue of 9% is observed. The residue may be due to the presence of γ-Fe_2O_3. The endothermic peaks observed in the DTA

trace at 127, 475, 500, and 564°C supplement the observations of the TGA trace.

Figure 2b shows the TGA/DTA trace of PEGA. This figure shows a steep and slow weight loss in the region from 50 to 415°C where a 7.2% weight loss is observed. Later a continuous weight loss is noticed in the temperature regions of 415 to 472 and 472 to 500°C, wherein weight losses of 37 and 44%, respectively, are observed. At 586°C, a residue of 11.7% remained. The amount of residue remaining is more than the amount of residue in the thermal trace of PEG. This is because of the presence of ash particles along with the γ-Fe_2O_3 present in PEGA. All endothermic peaks observed in the DTA trace at 125, 478, and 503°C supplement the observations made in the TGA trace of PEGA.

Figure 2c represents the TGA/DTA trace of PETUGA. This trace shows a steep weight loss in the temperature region of 34–420°C with a weight loss of 12.2%, and then from 420 to 471°C (II step) and 471 to 499°C (III step) continuous weight loss is observed with corresponding losses of 34.7 and 35%, respectively. At 589.78°C, a residue of 16.8% was observed. This is considerably higher than the residue observed for PEG and PEGA samples. This may be due to metal oxide, ash, char, and small undecomposed particles. All endothermic peaks observed at 127, 499, and 531°C supplement the observations made on the TGA trace of PETUGA.

Scanning electron microscopy

Figure 3a–c shows the SEM images of PEG, PEGA, and PETUG samples. Figure 3a shows the close packing of the knitted polymer network in which ultrafine particles of γ-Fe_2O_3 are dispersed. Because of the crystallinity achieved by the PEG composite film, the dispersion of γ-Fe_2O_3 looks slightly heterogeneous. Hence, the film processing was found to be difficult in the case of these samples. Figure 3b shows the SEM image of PEGA sample. Here also is observed the close packing of knitted polymer network along with fibrous ash particles dispersed in the HDPE matrix. Because of the presence of γ-Fe_2O_3 particles, the crystallinity increases and hence this film was also not easily processed. Figure 3c shows the SEM image of the PETUG sample. This shows the knitted polymer matrix in which the TUG complex is dispersed. Because of the crystallinity of the sample, the film processing was difficult. Therefore, it may be concluded that the presence of crystalline γ-Fe_2O_3 particles along with the thiourea complex increases the processing difficulty of these polymer composite films.

Dielectric study

Figure 4.1a–e shows the dielectric constant versus frequency curves for PE, PEG, PEGA, PETUG, and

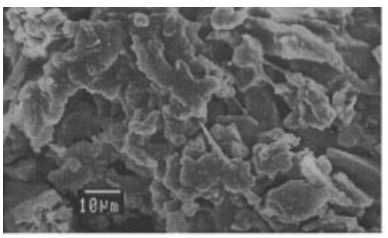

(a)

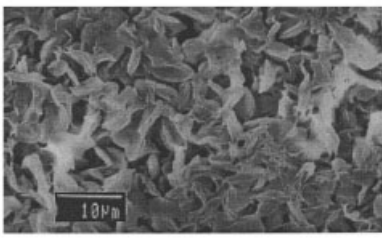

(b)

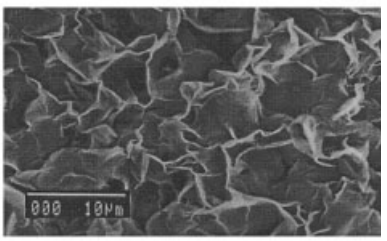

(c)

Figure 3 3a SEM image of PEG composite film. 3b SEM image of PEGA composite film. 3c SEM image of PETUG composite film.

PETUGA samples, respectively. All samples showed a general behavior of slow and gradual decrease in dielectric constant with respect to increase in frequency. The dielectric constant above 10^4 Hz remained constant for all these samples. This indicates that the additives like γ-Fe_2O_3, ash, γ-Fe_2O_3 and ash, TUG, TUG and ash, when added, have little effect on the dielectric behavior of HDPE. Hence, it may be believed that there is no induced dielectric polarization in the polymer matrix upon addition of the above-mentioned additives. These results are also supplemented by the similar nature of the dielectric loss versus frequency curves for the PE, PEG, PEGA, PETUG, and PETUGA samples shown in Figure 4.2a–e.

CONCLUSION

Processing of the HDPE composite films is not easy because of the crystalline nature of the additives, viz.,

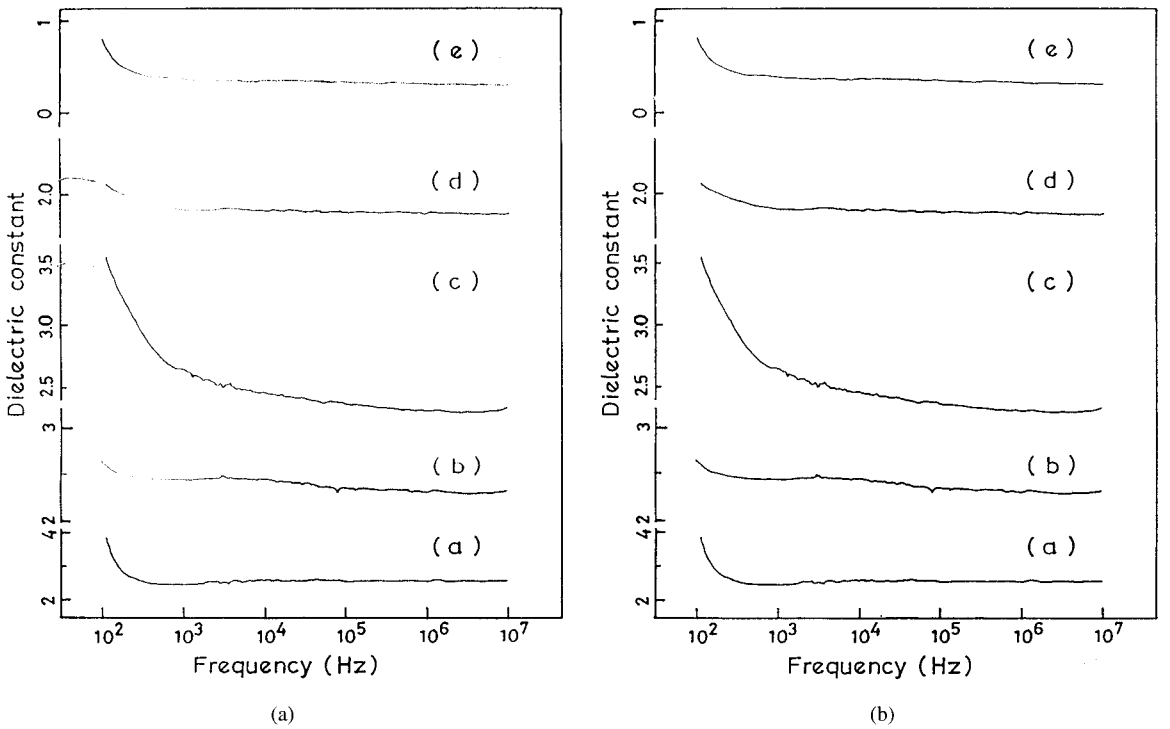

Figure 4 4A Dielectric constant behavior of (a) HDPE (PE) film, (b) PEG composite film, (c) PEGA composite film, (d) PETUG composite film, and (e) PETUGA composite film. 4B Dielectric loss behavior of (a) HDPE (PE) film, (b) PEG composite film, (c) PEGA composite film, (d) PETUG composite film, and (e) PETUGA composite film.

γ-Fe_2O_3, ash, and thiourea–γ-Fe_2O_3. The thermal stability of the polymer composites, especially with additives like ash and thiourea–γ-Fe_2O_3, increases and the presence of undecomposed matter as residue in the thermally treated composite was detected. The dielectric results indicate that there is no induced dielectric polarization in the HDPE matrix upon the addition of such additives as γ-Fe_2O_3, ash, and TUG.

Authors B. Govindraj and A. Venkataraman are grateful to the UGC, New Delhi, for financial assistance.

REFERENCES

1. Karch, J.; Birringer, R.; Gleiter, H. Nature 1987, 330, 556.
2. Gleiter, H. Prog Mater Sci 1989, 33, 223.
3. Gleiter, H. Adv Mater 1992, 4, 474.
4. Hahn, H.; Eastman, J. A.; Seigel, R. W. Ceram Trans 1998, B1, 1115.
5. Hahn, H. Nanostruct Mater 1997, 9, 3.
6. Mehta, P.; Singh, A. K.; Kingon, A. I. Mater Res Soc Symp Proc 1992, 242, 153.
7. Vollath, D.; Sickafus, K. E. Nanostruct Mater 1992, 1, 427.
8. Vollath, D.; Szabo, D. V. Nanostruct Mater 1994, 4, 927.
9. Vollath, D.; Szabo, D. V.; Seith, B. German Patent 19638601, 1997, 2.
10. Nieman, G. W.; Weertman, J. R.; Siegel, R. W. Scr Metall Mater 1990, 24, 145.
11. Siegel, R. W.; Ramasamy, S.; Hahn, H.; Li, Z.; Lu, T.; Gronsky, R. J Mater Res 1988, 3, 1367.
12. Jeon, K. S.; Lane, A. M. J Mag Mag Mater 1999, 193, 300.
13. Thrope, A. N.; Senftle, F. E.; Holt, M.; Grant, J.; Love, W.; Anderson, H.; Williams, E.; Monkres, C.; Brakett, A. J Mater Res 2000, 15(11), 2488.
14. Henglein, A. Chem Rev 1989, 89, 1861.
15. Wang, Y. Z.; Qiao, G. W.; Lu, X. D.; Ding, B. Z.; Hu, Z. Q. Mater Lett 1993, 17, 152.
16. Vollath, D.; Szabo, D. V.; Taylor, R. D.; Willis, J. O. J Mater Res 1997, 12, 2175.
17. Sun, T.; Garcés, J. M. Adv Mater 2002, 14(2), 128.
18. Usuki, A.; Kato, M.; Okada, A.; Kurauchi, T. J Mater Res 1993, 8, 1179.
19. Usuki, A.; Kawasumi, M.; Kojima, Y.; Okada, A.; Fukushima, Y.; Kurauchi, T.; Kamigaito, O. J Mater Res 1993, 8, 1185.
20. Kojima, Y.; Usuki, A.; Kawasumi, M.; Okada, A.; Fukushima, Y.; Kurauchi, T.; Kamigaito, O. J Appl Polym Sci 1997, 63, 137.
21. Barham, P. J. J Mater Sci 2000, 35, 5139.
22. Vonnegut, B. J. J Colloid Sci 1948, 3, 563.
23. Ross, G. S.; Frolen, L. J J Res Natl Bur Stand 1975, A79, 701.
24. Barham, P. J.; Jarvis, D. A.; Keller, A. J Polym Sci Polym Phys Ed 1982, 20, 1733.
25. Tudor, J.; Willingto, L.; O'Have, D. Chem Commun 1997, 2031.
26. Ramachandran, J.; Vivekanandan, S.; Lakshmi, S. Ind J Chem 2001, 40A, 105.
27. Venkataraman, A.; Mukhedkar, V. A.; Rahaman, M. M.; Nikumbh, A. K.; Mukhedkar, A. J. Thermochim Acta 1987, 112, 231.
28. Venkataraman, A.; Hiremath, V. A.; Date, S. K. Bull Mater Sci 2001, 24, 617.
29. Arunkumar, L.; Mallikarjuna, N. N.; Venkataraman, A. Ind J Chem Technol 2003, 10, 63.
30. Mallikarjuna, N. N.; Venkataraman, A. Talanta 2003, 60, 137.